Refinement of the EC stray radiation estimates for ITER

Franco Gandini

ITER Organization, Route de Vinon sur Verdon - CS 90 046 - 13115 Saint Paul Lez Durance, France

Abstract. The ITER ECRH&CD system is composed by 24 gyrotrons at 170 GHz that will deliver 20 MW at the plasma. Up to 6.7 MW will be injected in the empty vacuum vessel at the beginning of each plasma discharge to provide the gas breakdown. In that phase and when the plasma absorption is non ideal, a certain level of EC non-absorbed power, usually addressed as stray radiation, will be present. The EC stray radiation interaction with ITER first wall and diagnostics has been described in preliminary works. A more refined assessment is here described, following update of the diffuse stray radiation model and update of the launchers optics parameters. The optical design of the EC equatorial launcher has been entirely redesigned to optimize the power deposition and minimize interaction with the launcher structures. The updated parameters for the 24 launched beams are now available and have been used to estimate the interaction of the beams to be used for the breakdown phase with the tokamak structures. The preliminary stray radiation model described every opening of the tokamak as a "black" hole, that is a perfect power sink. Refining this crude description, using for the openings a "grey" hole model, provide a better agreement with benchmarks from other alternative models. Examples of stray radiation estimates performed for various ITER structures, systems and diagnostics are discussed.

1 Introduction

The ITER tokamak is equipped with an ECRH&CD (Electron Cyclotron Resonance Heating & Current Drive) system composed by 24 gyrotrons at 170 GHz, each one with 1 MW unit power (baseline value). Each source is connected to an equatorial launcher (EL, installed in Port 14) and one of the upper launchers (UL, installed in Ports 12, 13, 15 and 16). The EL is used for central heating and current drive applications with a deposition range covering $0< \varrho_T <0.6$ (where ϱ_T is the square root of the toroidal flux). The UL is used for control of magnetohydrodynamic (MHD) activity such as the neoclassical tearing mode (NTM) and sawtooth oscillation with a deposition range covering $0.4< \varrho_T <0.88$. The access ranges of each steering mirror are different for all launchers. This is particularly the case for the UL in which the upper steering mirror (USM) is used to access the inner region of the plasma for controlling sawtooth and q=3/2 NTMs, while the lower steering mirror (LSM) is used to control the q=3/2 and 2 NTMs. For what concern the equatorial launcher, three steerable mirrors collecting the RF beams delivered from eight waveguides are installed at the bottom of the shield slots. The beams are injected in a fixed toroidal direction and can sweep vertically from -30° to +30° by rotation of the steerable mirror. One mirror directs its 8 beams in the counter-current drive direction (cnt-ECCD, clockwise looking from the top, from port 14 towards ports 13, 12, 11, etc.) while the other two mirrors direct their 8+8 beams in the co-current drive direction (co-ECCD, counter-clockwise looking from the top, from port 14 towards ports 15, 16, 17, etc.). About the upper launchers, each one has 8 beams in input, 4 routed to the upper steering mirror and 4 routed to the lower steering mirror. The beams can sweep vertically from about -23° to about -68° by rotation of the steerable mirror. The precise angle range depends on the launching mirror (see table 1 for a summary of the functions and the steering capability of both launchers type).

Table 1. Summary of launcher design parameters

Type	
Equatorial Launcher	Upper Launcher
Functions	
1. Plasma heating and access to H-mode. 2. On- & off-axis CD for steady state operation. 3. Initial breakdown for plasma start up.	1. Plasma heating and access to H-mode. 2. Off-axis CD mainly for NTM stabilization. 3. Initial breakdown for plasma start up.
Ports	
Equatorial 14	Upper 12, 13, 15 & 16
Injected power	
Up to 20 MW/port	Up to 6.7 MW/port
Frequency	
170 GHz	
beam steering capability (α: poloidal, β: toroidal)	
Top mirror α = ±10° β = 20° cnt-ECCD Middle mirror α = -5° ÷ -30° β = 25° co-ECCD Bottom mirror α = 10° ÷ 30° β = 25° co-ECCD	Upper Steering Mirror α = -28° ÷ -68° β = 15° ÷ 22° co-ECCD Lower Steering Mirror α = -23° ÷ -60° β = 17° ÷ 21° co-ECCD

1.1 Operating modes

To accomplish the design scopes of the EC system there are critical phases characterized by low absorption and therefore high levels of stray radiation that could harm tokamak structures:

1.1.1 Breakdown

Up to 6.7 MW of EC power are going to be injected in the "empty" ITER chamber at the beginning of discharge in order to assist gas ionization and plasma formation (breakdown). In this phase there is no RF power absorption from the plasma, only absorption from the wall at the points where the beam is reflected and, after some bounces, diffuse radiation that can escape from the chamber openings. The wavelength in vacuum of the EC radiation is 1.76 mm, therefore any aperture larger than 0.8 mm can be considered as an "escaping opening".
The expected duration of this phase is no longer than few seconds, with the EC power injected by burst of no more than 300 ms.

1.1.2 Burn through (total EC power injected: up to 6.7 MW)

It is the phase after initial ionization and breakdown, when a current channel forms and the discharge is heated. In this phase the radiation from low Z impurities must be lower than the injected power to successfully evolve the discharge to the current ramp up phase. Moreover, in this phase the power injected to compensate the radiation from impurities is not significantly absorbed by the plasma and the power loading for the chamber wall is of the same kind described at the previous point.

The expected duration of this phase is few seconds (nominally 5.5 seconds). The amount of power to be used will be assessed during the PFPO1 operational phase.

1.1.3 HCD with non-optimum polarization (total EC power injected: up to 20 MW)

The absorption of EC waves is optimized only when injected with the correct polarization. Any error in polarization would mean additional stray radiation. The fraction injected with the wrong polarization will undergo strong diffraction and/or reflection at the cut off layer. The correct description of this effect requires a beam tracing calculation. A qualitative estimate of the power deposition can be obtained evaluating the beam size of the cross polarized fraction of the injected beam at the possible incidence point and the power density dividing the power in the wrong polarization by the projected area of the beam.
Without the control of the effective injected polarization, a conservative assumption is that the stray power coming from non-optimum polarization will be present through the whole discharge.

2 Description of the residual Power

When the plasma absorption is poor or negligible, it is assumed that the structure of the injected astigmatic Gaussian beams is maintained at least through the first 3 bounces: this assumption is a simplification to over-estimate the peak power deposition and the average power loading on the chamber wall from the collimated beam (shine through). Also, the wall structure and shape are not taken into account: the wall is described as a plane perfect reflector. After some reflections we assume that the radiation inside the tokamak chamber cannot be anymore described as a collimated beam but, on the contrary, it may be described as diffuse (stray) radiation.

2.1 Shine through

The breakdown and burn through assistance require up to 6.7 MW injected from the equatorial launcher. The following results have been obtained considering the injection of 8 beams (0.8375 MW each) from the top steering mirror of the equatorial launcher (port 14). As zero order assumption, the exact vertical locations of the mirror (z = 0.04 m) is neglected, and the beams are considered to come from the equatorial plane z = 0 and propagate in the horizontal plane (see Fig.1).

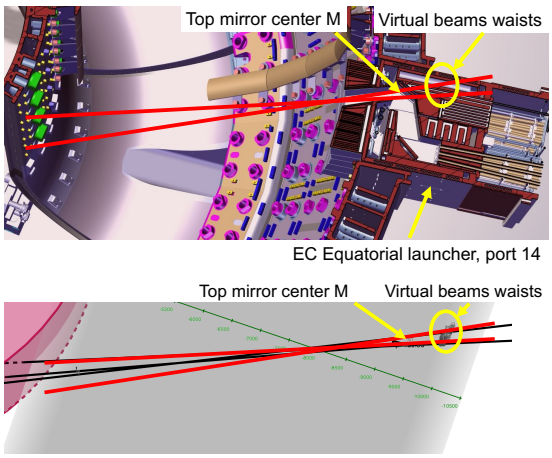

Fig. 1. Launching scheme from the top mirror of port equatorial 14: above, cross section of launcher and vacuum vessel; below, geometrical representation of the beams.

The following assumptions are considered:

- Pure gaussian propagation from virtual waists locations (Fig. 2)
- Central column represented as cylindrical surface at R=4.0 m
- Low field side wall (LFSW) represented as cylindrical surface at R=8.5 m
- Mirror-like reflections at tangential plane at beam axis incident points (Fig. 3)
- Merged beams described as gaussian (conservative assumption, Fig. 5)

The eight beams are followed individually. The beams are considered merged (to simplify the analysis) when, at the reflection's locations, they are close enough.

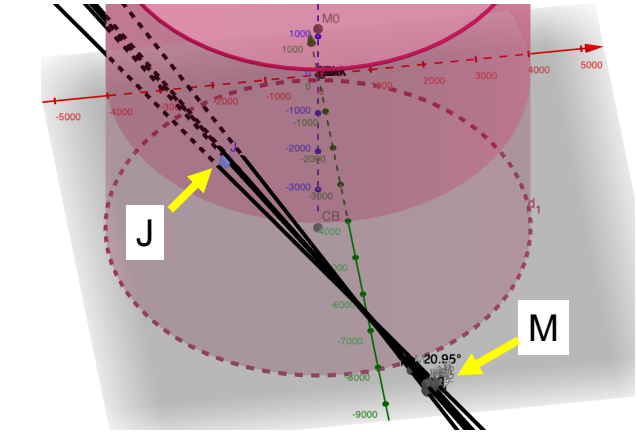

Fig. 2. Beams propagated from their virtual waist location along their **k** vectors, estimated path length from waists area to the central column (7.3 m), identified point "J" at 6.6 m from "M"

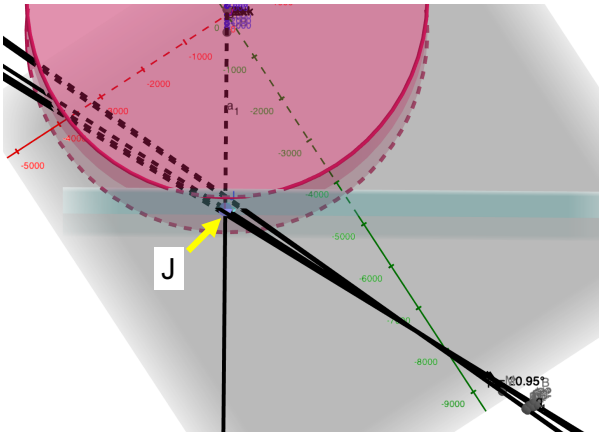

Fig. 3. Built plane in "J" tangential to the central column

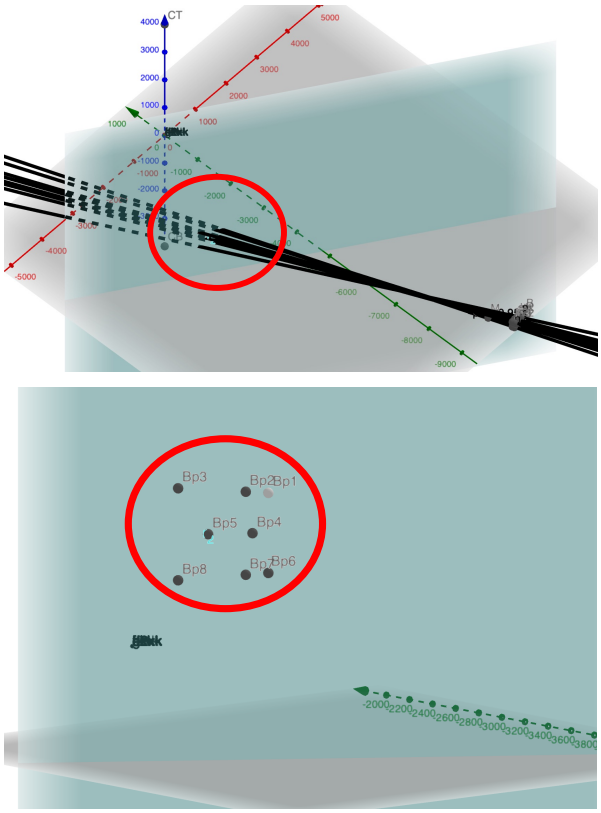

Fig. 4. Incident points of the 8 beams **k** vectors

Fig. 5. Incident points of the 8 beams. The beams considered merged are the ones incident at (Bp1-Bp2), (Bp4-Bp5) and (Bp6-Bp7)

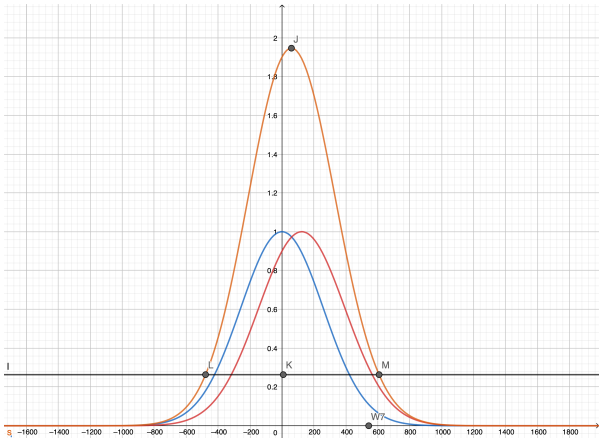

Fig. 6. Beams at (Bp1-Bp2) and (Bp6-Bp7) superposed in the horizontal direction, The distance (Bp1-Bp2) and (Bp6-Bp7) is 124 mm

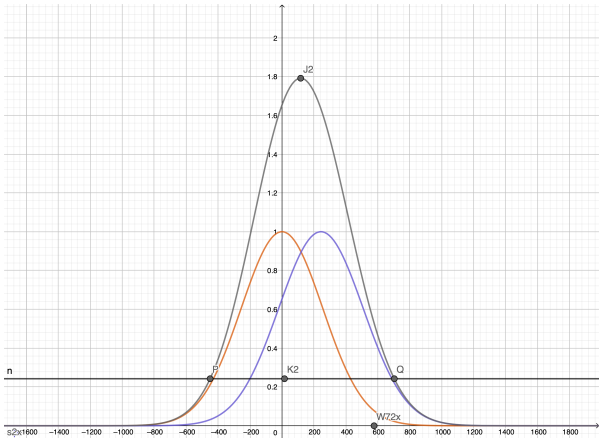

Fig. 7. Beams at (Bp4-Bp5), distance 244 mm, superposed in the horizontal direction

The six beams (Bp1+Bp2), (Bp6+Bp7) (see Fig. 6) and (Bp4+Bp5) (see Fig. 7), once merged horizontally and described as gaussian beams, are then further merged vertically. The beam sizes (radius at 1/e, projected on the plane tangential to the central column) are: (Bp1+Bp2) and (Bp6+Bp7) 543 mm horizontally and

224 mm vertically; (Bp4+Bp5) 577 mm horizontally and 214 mm vertically.

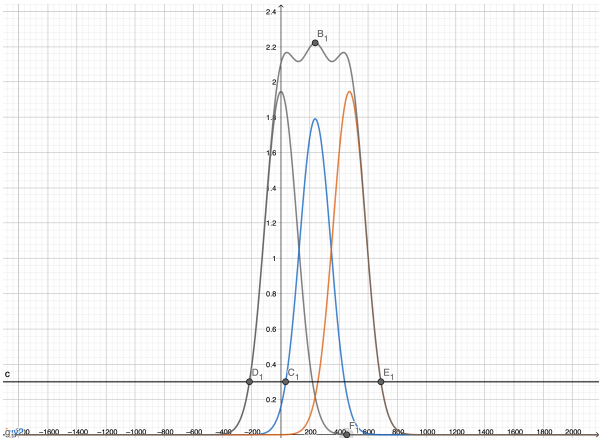

Fig. 8. Beams (Bp1+Bp2), (Bp6+Bp7) and (Bp4+Bp5) superposed in the vertical direction

Finally, the six beams are described as a superposed astigmatic gaussian beam with sizes W_x = 565 mm horizontally and W_y = 451 mm vertically (see Fig. 8). The peak intensity is calculated as

$$P_{axis}=(2\,P_{in})/(\pi\,W_x\,W_y) \quad (1)$$

where P_{in} is the six beams merged input power and P_{axis} is the power density on the axis. The average power density P_{aw} is estimated considering the whole transmitted power distributed over the projection of the merged beam on the chamber wall at the reflecting points

$$P_{aw}=P_{in}/(4\pi\,W_y\,W_x/\cos\alpha) \quad (2)$$

where α is the merged beam incident angle. The same analysis can be extended to the next reflection at the low field side (Fig. 9)

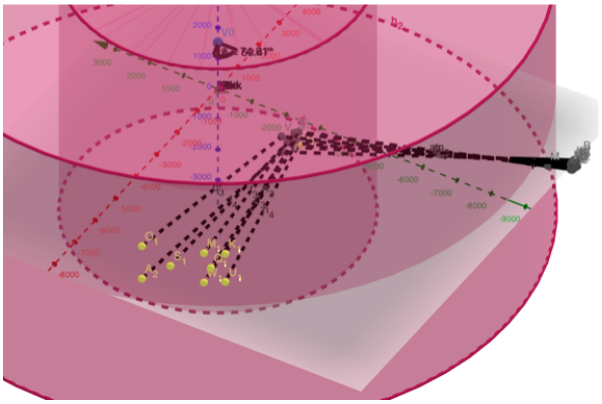

Fig. 9. Incident points at low field side, second reflection

Considering EC-assisted breakdown from the ECH Equatorial launcher (8 beams injected from the same mirror for a total power of 6.7 MW), the expected incident peak power density at the first bounce location on the HFS wall is about 13 MW/m² (but just on the beam axis), with absorption of about 1% in the wall itself (absorbed peak power: 0.13 MW/m²). The average incident power loading is 1.6 MW/m² (absorbed average power: 0.016 MW/m²). The second bounce is in the area between port 10 and port 11 (see Fig. 10) and the expected peak power is about 3.8 MW/m² (again, to be considered only on the beam axis), while the average power loading is 0.5 MW/m². To be considered that the beams footprint at the second bounce is quite large, with a projected horizontal beam size W_x = 767 mm and a vertical beam size W_y = 928 mm, for a 4w beam area of nearly 9 m².

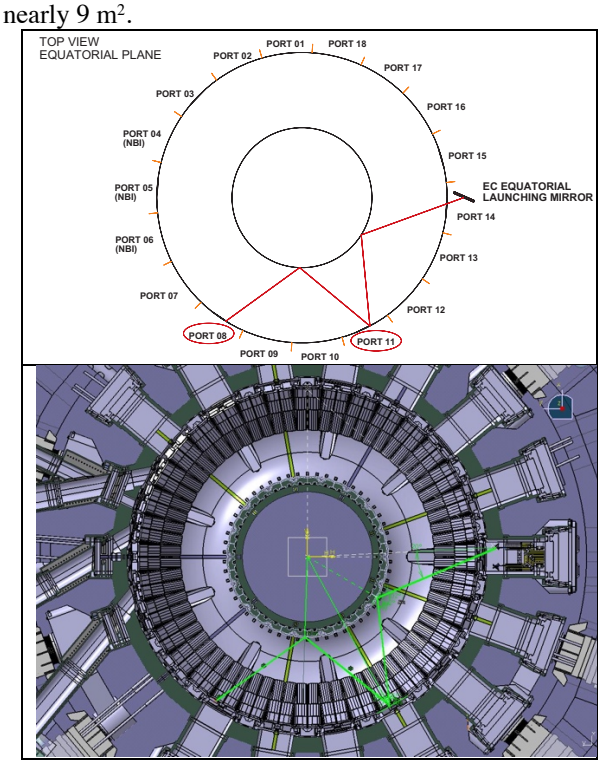

Fig. 10. First reflection locations for beams injected from equatorial port 14: above, geometrical representation of the beams; below, top view of tokamak equatorial plane section.

These results have been obtained considering the refined equatorial launcher beams parameters and significantly relax the previous loads that were calculated using the preliminary beams parameters [1]: the previous P_{axis} at the first bounce was 334 MW/m², while the P_{aw} was 25 MW/m².

Table 2. Summary of incident peak power density P_{axis} and average power density P_{aw} for the first two bounces

1st bounce		2nd bounce	
P_{axis} MW/m²	P_{aw} MW/m²	P_{axis} MW/m²	P_{aw} MW/m²
13	1.6	3.8	0.5

2.2 Diffuse stray radiation

After few reflections on the tokamak walls, it is assumed that the injected power loses its beam structure and a diffuse, more or less isotropic background level of stray radiation is established. A simplified description of the behaviour of the stray radiation in the chamber can be developed from the integrating sphere theory, a concept that has been developed to describe the input/output radiation ratio in a sphere with finite reflectivity ρ and multiple openings [2, 3]. The simplest version of the model considers the reflective surfaces having all the same reflectivity and all the openings as perfect absorbers (black holes):

$$\tau_{BH}=\frac{A_i}{A_s}\frac{\rho}{1-\rho\left(1-\frac{\sum A_i}{A_s}\right)} \quad (3)$$

where τ_{BH} is the throughput of the sphere ("black hole" case), i.e., the ratio of the exiting flux from a test opening (the "exit opening") to that entering the sphere. A_i is the exit opening area; A_j is the summation of all the openings areas and A_s is the area of the sphere. However, most of the large opening considered (equatorial and upper ports openings, divertor gap, NBI ports) have a complex structure and describe them as "black" hole is not completely justified. The results from the preliminary work [1] ("black hole" model) have been compared with alternative modeling [4, 5], and a good agreement can be achieved including a term in the equation and treat the openings as "grey", attributing them a reflection coefficient ρ_G:

$$\tau_{GH} = \frac{A_i}{A_s} \frac{\rho}{1-\rho\left(1-\frac{\Sigma A_j}{A_s}\right)-\rho_G\frac{\Sigma A_j}{A_s}} \quad (4)$$

A_s = Total surface area = 858.3 m²
ΣA_j = Total opening surfaces = 43.5 m²
ρ = Wall reflectivity = 0.99 average

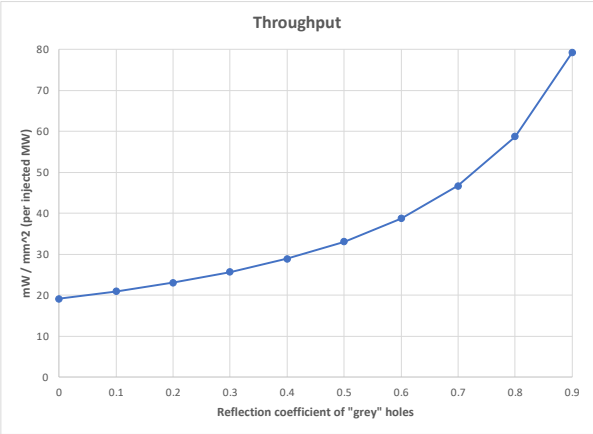

Fig. 11. Output flux (throughput) from a small opening as function of "grey" hole's reflection coefficient

A conservative preliminary assumption is to consider an average reflection coefficient $\rho_G = 0.6$ for the openings and therefore a throughput of about 40 mW/mm² per injected MW (Fig. 11).
In the tables 3 and 4 are reported few examples of expected output flux from some openings and behind the blankets during the breakdown phase (6.7 MW injected in the empty chamber).

Table 3. expected output flux from some openings during the breakdown phase (6.7 MW injected in the empty chamber)

	Opening surface m²	Output flux (kW) black holes 20 mW/mm²	Output flux (kW) grey holes 40 mW/mm²
NBI large port	1.19	160	319
Reflectometer (LFS, EqP11) ϕ31.75 mm	0.00079	0.10	0.21
Reflectometer (LFS, EqP11) ϕ50.8 mm	0.0020	0.27	0.54
Reflectometer (LFS, EqP11) ϕ63.5 mm	0.0032	0.43	0.86
Reflectometer (LFS, EqP11) ϕ88.9 mm	0.0062	0.83	1.66

Table 4. power to be expected diffused behind the blanket modules

	mW/mm² per injected MW Black holes	mW/mm² per injected MW Grey holes
HFS – mod 1÷5 – vertical and horizontal gaps	4.5	9.0
HFS – modules 6÷7 – vertical gaps	8.6	17.2
HFS – modules 6÷7 –horizontal gaps	6.1	12.2
LFS – vertical and horizontal gaps	16.7	33.4

3 Conclusion

The model here described is a simplification of reality with the purpose of providing a conservative assessment of the expected level of EC incident power on the central column and on the Low Field Side Wall (LFSW).
The real surface of the Blanket panels at the central column is different from an ideal cylinder and even more different from a plane: the reflected beams from such shaped surface will diverge more than considered here, lowering the power density at LFSW.
The merged beams are described as they would have gaussian shape, as consequence both the peak power and the average power density are overestimated.
For a more realistic assessment of the wall loading is needed a beam tracing and accurate model of the reflecting wall shape.
The updated parameters for the 24 launched beams have been used to estimate the interaction of the beams to be used for the breakdown phase with the tokamak structures.
The preliminary stray radiation model described every opening of the tokamak as a "black" hole, that is a perfect power sink. Refining this crude description using for the openings a "grey" hole model provides a better agreement with benchmarks from other alternative models.

The views and opinions expressed herein do not necessarily reflect those of the ITER Organization

References

1. F. Gandini, M. Henderson, C. Nazare, C. Darbos, T. Gassmann, D. Purohit, and T. Omori , "Stray RF Power Estimates From EC Exploitation During ITER Plasma Operations", AIP Conference Proceedings 1406, 173-176 (2011) https://doi.org/10.1063/1.3664955
2. D. G. Goebel, "Generalized Integrating-Sphere Theory", *App. Opt.* **6**, n.1, 125-128 (1967).
3. D. J. Lovell, "Theory and Application of Integrating Sphere Technology", *Laser focus/Electro-optics*, 86-96 (1984)
4. D. Moseev, J.W. Oosterbeek, A. Sirinelli, Y. Corre, M. Houry, S.B. Korsholm, H.P. Laqua, S. Marsen, M. Preynas, J. Rasmussen, M. Salewski, T. Stange, V. Udintsev, *Stray radiation energy fluxes in ITER based on a multiresonator model*, Fusion Eng. Des., **172**, (2021), 112754, ISSN 0920-3796, https://doi.org/10.1016/j.fusengdes.2021.112754
5. J. Oosterbeek, V.S. Udintsev, F. Gandini, M. Hirsch, H.P. Laqua, N. Maassen, Y. Ma, A. Polevoi, A. Sirinelli, G. Vayakis, M.J. Walsh, *Loads due to stray microwave radiation in ITER*, Fusion Eng. Des., **96–97**, 553-556 (2015), ISSN 0920-3796, https://doi.org/10.1016/j.fusengdes.2015.05.068